J. Membrane Biol. 75, 241–251 (1983)

The Journal of
Membrane Biology

Potassium Channels in the Membrane of *Hydrodictyon africanum*

G.P. Findlay and H.A. Coleman
School of Biological Sciences, The Flinders University of South Australia, Bedford Park, South Australia, 5042, Australia

Summary. The potential difference across the membrane of *Hydrodictyon africanum* was controlled by voltage clamping and positive and negative steps in the PD were applied. For positive steps in the PD to values less negative than a threshold value, there is a PD and time-dependent increase in the outward current which has an S-shaped time course. Following the cessation of these steps, the current reverses instantaneously and declines with a simple time course. These currents show a strong K^+ dependence and are blocked by tetraethylammonium (TEA) and nonyltriethylammonium (C_9) ions, suggesting that they arise from the opening and then the closing of K^+ channels. There is also a PD and time-dependent increase in the inward currents in response to negative steps in the membrane PD. The membrane properties have been described by three current-voltage curves, for the instantaneous current, for the steady-state current and for the current flow when the K^+ channels are open. The response of the unclamped or free-running membrane PD to steps of constant current can be accounted for by the observed kinetics of the opening and closing of the K^+ channels.

Key Words K^+ channels · *Hydrodictyon* · membrane · TEA effects

Introduction

The presence of voltage- and time-dependent potassium channels in various types of animal cell membranes (Armstrong, 1975) and artificial phospholipid membranes (Muller & Finkelstein, 1972) is well established. The membrane potassium conductance, g_K, which measures the fraction of open channels does not change instantaneously when the membrane PD is changed in a stepwise fashion, but exhibits characteristic and different time courses for channel opening and channel closing. For opening, g_K rises in an S-shaped curve to a steady level, and for closing, g_K falls exponentially to a steady level.

There is considerable evidence that g_K forms a major part of the total diffusive ionic conductance of plant membranes, from early work by Osterhout (1930) and Hill and Osterhout (1938) on the membrane of *Nitella,* to recent work by Smith and Walker (1981) and Keifer and Lucas (1982) on *Chara* and Findlay (1982) on *Hydrodictyon.* However, there do not appear to be published data of separate potassium currents flowing during voltage-clamped steps in membrane PD. In voltage-clamp data from *Chara* (Bielby & Coster, 1979), the potassium current is obscured by the transient chloride current.

Findlay (1982) has shown that in *Hydrodictyon africanum,* g_K can have either a high or low value depending on whether the membrane PD, ψ_m, is less negative or more negative than a threshold level, ψ_{th}. Various factors which change ψ_m and move it across ψ_{th} cause g_K to change value, not instantaneously, but over times of up to 100 sec. In these types of measurement, however, the membrane PD was not clamped, but allowed to free run, and thus no specific information was obtained about the time and voltage-dependence of g_K, with ψ_m as the independent variable. To obtain this information, we have performed voltage-clamp experiments in which the membrane PD in *Hydrodictyon africanum* was moved in stepwise fashion between various levels and the resultant membrane currents measured. The results of these experiments are described in this paper.

Materials and Methods

Materials

Coenocytes of *Hydrodictyon africanum* were grown in continuous light, in sterile culture, either under stagnant conditions or bubbled with a mixture of air and CO_2. The stagnant cultures were maintained at 15 °C in 1-liter Ehrlenmeyer flasks. These culture vessels were prepared by autoclaving 100 g of washed acid sandy loam in 500 or 1000 ml of a solution consisting of either (in mM): (a) KNO_3, 0.17; $MgSO_4 \cdot 7H_2O$, 0.07; K_2HPO_4, 0.1; K_2CO_3, 0.14; $CaNO_3$, 0.28; together with trace elements, or (b) KNO_3, 1.0; $MgSO_4 \cdot 7H_2O$, 1.0; Na_2HPO_4,

0.1; NaH_2PO_4, 0.5; $CaCl_2$, 0.1; Fe EDTA, 0.002; together with trace elements, and were left to stand for several days to allow fine suspended matter to settle. The starting materials for the cultures were either zygotes or small nets from the Cambridge algal collection, or zygotes or groups of small cells from previous cultures. The bubbled cultures were maintained at ~22 °C in vertical glass tubes of diameter 50 mm, with a mixture of air and some added CO_2 bubbled from the bottom. The culture medium was solution (b), above, without any added loam. In this bubbling culture, the nets tended to break up at an early stage and finally produced single spherical cells up to 2 to 3 mm in diameter. The growth rate of cells was quite high, cells increasing in diameter from about 0.2 to 2.0 mm in 3 to 4 weeks. However, the cells often did not survive more than 4 to 6 weeks in this culture, and were usually transferred to a stagnant culture, with solution (a) above, after 3 to 4 weeks, with 16 hr of continuous illumination per day.

Samples of vacuolar sap for analysis of ionic content were obtained by first soaking the cells in a solution of 10 mM $CaCl_2$ for 30 sec to remove extracellular Na^+ and K^+. The cells were then blotted dry, and cut open with a sharp razor blade on a greased surface. A 5 to 10 µl sample of vacuolar sap was then collected and added to 2 ml of distilled water for determination of K^+ and Na^+ concentrations by flame photometry.

Methods

We aimed, in these experiments, to use cells in which the membrane was hyperpolarized, i.e. the membrane PD was more negative than any possible ion diffusion PD. In such cells, the electrogenic hydrogen efflux pump is operating and the diffusive conductance is low (Findlay, 1982). To this end cells were soaked overnight in the light in a solution consisting of (in mM) KCl, 0.1; $CaCl_2$, 0.1; $NaHCO_3$, 0.3; TAPS (3-[[tris-(hydroxymethyl)methyl]amino] propane sulfonic acid), 4.0, adjusted to pH 8.5 with NaOH ~2.4. This pretreatment often, but not always, produced cells that were in the hyperpolarized state at the start of experiments. The pretreatment solution also formed the basic control solution. Changes in $[K^+]_o$ were usually made by increasing the concentration of KCl in the solution.

The cells were mounted in a Perspex® holder, allowing irrigation with continuously flowing solution, and immobilized by being gently pushed into a V-shaped section by a flat-ended glass rod. The light from the viewing microscope provided illumination.

The membrane PD, ψ_m, was measured with a unity-gain differential amplifier, between an inserted 3 M KCl-filled micropipette (with internal capillary fiber; blanks supplied by Clark Electromedical) and an agar-KCl salt bridge in the external solution. Electrical connection between the internal micropipette and the external reference electrode was made through a balanced pair of Calomel half-cells. The measured PD was assumed to be the PD across the plasmalemma of the cell; *see* Findlay (1982) for further information on this point. The bath was held at virtual earth by a current-to-voltage amplifier with feedback resistance of 2 to 100 kΩ.

Electric current was injected into the cell either through a 3 M KCl-filled micropiette, or a glass insulated metal electrode. The KCl-filled current micropipette was used for some of the earlier experiments, but its resistance was often too high, the current flow limited, and the voltage-clamp control of membrane PD not always satisfactory. The metal electrode consisted of a Pt−Ir alloy wire with glass insulation. Up to 50 µm of the metal was exposed, and electropolished to a sharp point. At the surface of the cell, the diameter of the insulated electrode was about 15 to 20 µm. For details of construction methods *see* Findlay and Hope (1964). The low resistance of these electrodes usually allowed sufficient current flow for satisfactory voltage-clamp control of the membrane PD.

The voltage-clamp system was similar to that described by Bielby and Coster (1979) and Findlay and Hope (1976), but the feedback amplifier had a maximum output of ±150 V, and could operate in the clamp circuit with a gain of up to 2000. Usually the membrane PD could be controlled to within ±1.5 mV of the set level, and took about 2 msec to reach a new level following a step in the "command" voltage. We did not correct the voltage-clamp data for the effect of the extracellular resistance, because usually the cell resistance was very much larger than the extracellular resistance. Pulses of constant current were injected into the cell from a pulse generator, providing up to ±250 V, through a resistance of 10^8 Ω. Membrane currents and PD's were displayed on a double-channel pen recorder (Rikadenki) and a double-channel storage oscilloscope (Tektronix) and stored on magnetic tape for subsequent analysis.

As most of the cells were approximately spherical, the diameter was estimated as the mean of two orthogonal diameters, and the surface area calculated accordingly.

The TEA and C_9 cations were provided by tetraethylammonium chloride (B.D.H.) and nonyltriethylammonium bromide (Polysciences), respectively.

Results

Membrane Currents

In the cells studied, the membrane PD was clamped at a holding value of −175 to −200 mV. In most of the cells this value was close to the resting PD while in the remainder the value was more negative than the resting PD by up to 50 mV. The membrane PD was changed from the holding level in steps of alternating sign and increasing magnitude, lasting for up to 6 sec at time intervals sufficiently long to allow the current to return to its initial level between each step. The membrane current I_m flowing in response to a series of steps is shown in Fig. 1. For voltage-clamp steps which shift ψ_m to less negative values the membrane currents are outward, and for ψ_m above a threshold level, I_m after a short delay rises in a characteristic S-shaped curve, and reaches a steady level in ~2 to 4 sec (Fig. 1 *a, b*). For steps in ψ_m to values more negative than the holding potential I_m is inward and shows some time dependence, usually an increase with time to a steady level (Fig. 1 *c*). At the end of the positive step in ψ_m, provided ψ_m was less negative than ψ_{th}, I_m showed a characteristic "tail" in which the current instantaneously reversed, and then decreased with time to the original holding level. The magnitude of the tails approached a maximum value as ψ_m was stepped to progressively less negative values. At the end of negative steps in ψ_m, I_m returned, usually without reversal, to its original holding level.

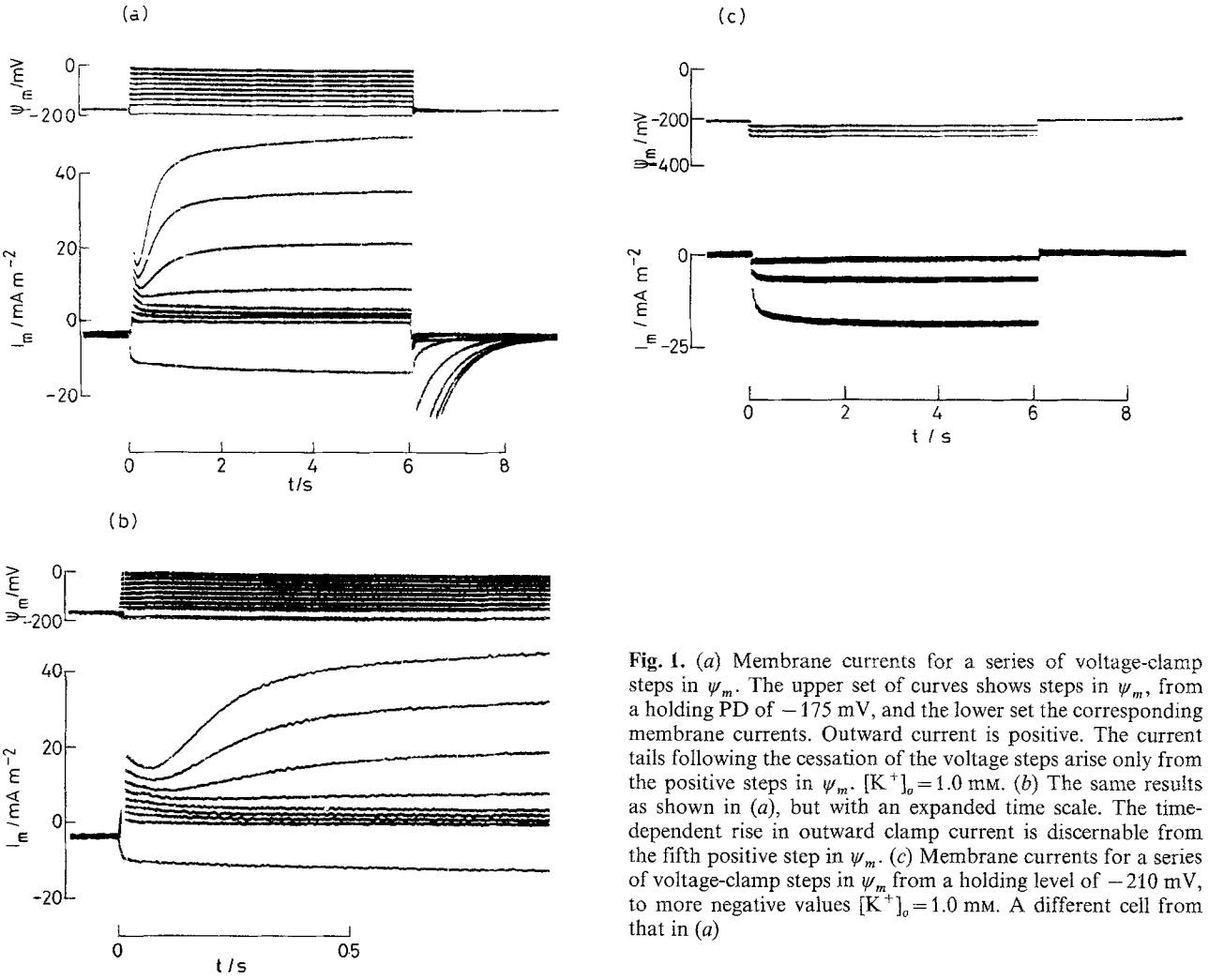

Fig. 1. (*a*) Membrane currents for a series of voltage-clamp steps in ψ_m. The upper set of curves shows steps in ψ_m, from a holding PD of −175 mV, and the lower set the corresponding membrane currents. Outward current is positive. The current tails following the cessation of the voltage steps arise only from the positive steps in ψ_m. $[K^+]_o = 1.0$ mM. (*b*) The same results as shown in (*a*), but with an expanded time scale. The time-dependent rise in outward clamp current is discernable from the fifth positive step in ψ_m. (*c*) Membrane currents for a series of voltage-clamp steps in ψ_m from a holding level of −210 mV, to more negative values $[K^+]_o = 1.0$ mM. A different cell from that in (*a*)

We have defined the following components of the measured clamp current: (a) I_1, the membrane ionic current 100 to 200 msec after the start of the step. This is at a time after the cessation of the capacitative current caused by the step change in $\psi_m (I_M = C_m \partial \psi_m / \partial t$, where C_m is the membrane capacitance), and before the S-shaped rise in the outward current. (b) I_2, the steady current at times after about 6 sec from the start of the step. (c) I_3, the membrane ionic current 100 to 200 msec after the end of the step.

In another series of experiments, we examined the PD dependence of the magnitude and decay of the tail current by applying a double step to ψ_m. The first step, shifting ψ_m to a value less negative than the holding potential was set at a level that produced an approximately maximum tail current if ψ_m was returned directly to its holding level. This first step was applied until I_m reached its steady value ($= I_2$). The level of the second step was varied over a range of values more negative than the first step; *see* Fig. 2. During the second step, I_m decreases to a new steady level, but with a complex time course; not a single exponential, although the curve can often be fitted by the sum of two exponential functions. The overall rate at which I_m approaches its new steady level increases as ψ_m becomes more negative. In this series of clamp currents, I_3 was measured immediately after the end of the first step.

$I \sim \psi_m$ Curves

Typical relationships between I_1, I_2 (from Fig. 1), I_3 (from Fig. 2), and ψ_m are shown in Fig. 3. The PD at which the $I_3 \sim \psi_m$ curve intersects the $I_1 \sim \psi_m$ curve we call ψ'_m. Figure 4 shows current-voltage curves for three different values of $[K^+]_o$; 0.1, 1.0 and 10.0 mM on Fig. 4. The essential feature to note is that the $I_2 \sim \psi_m$ and $I_3 \sim \psi_m$ curves are shifted to the right as $[K^+]_o$ is increased. In 22 cells studied, $\psi_{m(I_2=0)}$, for $[K^+]_o = 0.1$ mM, ranged

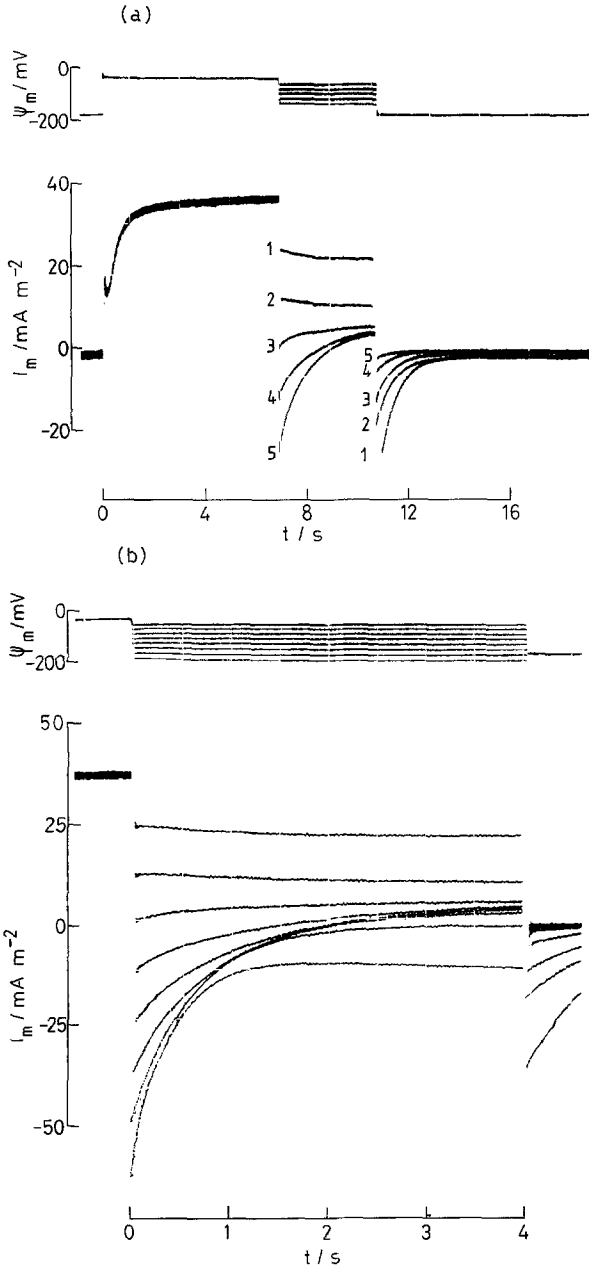

Fig. 2. (*a*) Membrane currents during a voltage-clamped double-step sequence. The membrane PD was stepped from a holding PD of −175 mV to a prepulse level of −35 mV, and then stepped to the various levels as shown. Five current traces are superimposed. The numbers near the separate curves identify each current response. $[K^+]_o = 1.0$ mM. (*b*) The same results as in (*a*), on an expanded time scale, and with the oscilloscope traces triggered just before the end of the prepulse. The currents flowing during three extra steps in ψ_m are included. The lowest two steps have taken ψ_m below the holding PD. The results shown in this Figure, and in Fig. 1 *a*, came from the same cell

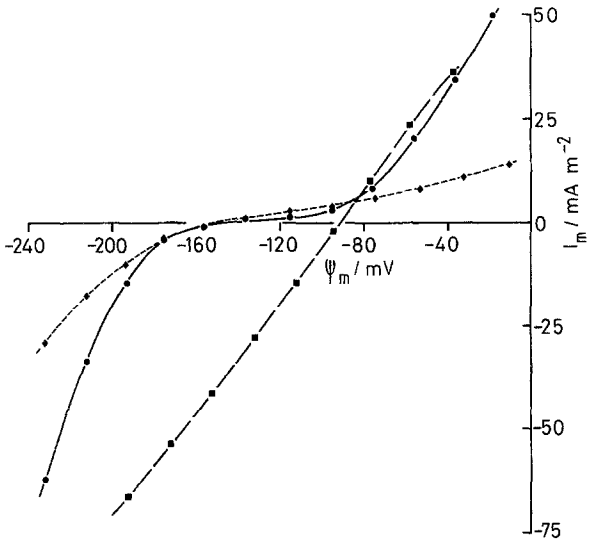

Fig. 3. The membrane currents I_1, I_2 and I_3 as functions of ψ_m. The $I_1 \sim \psi_m$ (♦) and $I_2 \sim \psi_m$ (●) curves are from the data shown in Fig. 1, and the $I_3 \sim \psi_m$ (■) curve from the data shown in Fig. 2. The curves have been drawn by eye. Further details are in the text

from −220 to −100 mV, and $(\partial I_2/\partial \psi_m)_{I_2=0}$ ranged from 0.048 to 1.4 S m^{-2} with the functional relationship between these two parameters similar to that found by Findlay (1982) for resting membrane PD and conductance. In 16 of the cells, ψ_m was more negative than −149 mV, and $(\partial I_2/\partial \psi_m)_{I_2=0}$ was low, with a mean value of 0.125 ± 0.012 S m^{-2}. Up to 6 of these cells also yielded results with $[K^+]_o = 1.0$ to 10.0 mM. The parameters $(\psi_m)_{I_2=0}$, $(\partial I_2/\partial \psi_m)_{I_2=0}$, $(\partial I_1/\partial \psi_m)_{I_3=I_1}$, $(\partial I_3/\partial \psi_m)_{I_3=I_1}$, $(\psi_m)_{I_3=I_1} (= \psi'_m)$ and $[K^+]_{i,\text{calc.}}$ as functions of $[K^+]_o$ are shown in the Table. $[K^+]_{i,\text{calc.}}$ is the value of the internal K^+ concentration calculated from the Nernst equation, $\psi_K = 58 \log \{[K^+]_o/[K^+]_i\}$, on the assumption that $\psi_K = \psi'_m$; *see* later discussion. In two groups of cells (taken from the same cultures as the experimental cells) the vacuolar concentrations of K^+ and Na^+, measured by flame photometry, were $[K^+]_v = 11.05 \pm 0.99$ (6) mM, $[Na^+]_v = 6.17 \pm 0.79$ (6) mM and $[K^+]_v = 19.22 \pm 1.22$ (5) mM, $[Na^+]_v = 8.12 \pm 0.39$ (5) mM.

The Free-Running Membrane PD

The responses of the free-running membrane PD to constant current steps are shown in Fig. 5. When $[K^+]_o = 1.0$ mM (Fig. 5 *a*), ψ_m for the first few current steps changed with an exponential time course at the start and finish of the pulse. For a sufficiently large current step an initial peak in ψ_m became apparent at about 200 msec from the start of the step and then occurred at progressively shorter times as the magnitude of the current step was increased. Associated with the appearance of the peak is the occurrence of a plateau in the recov-

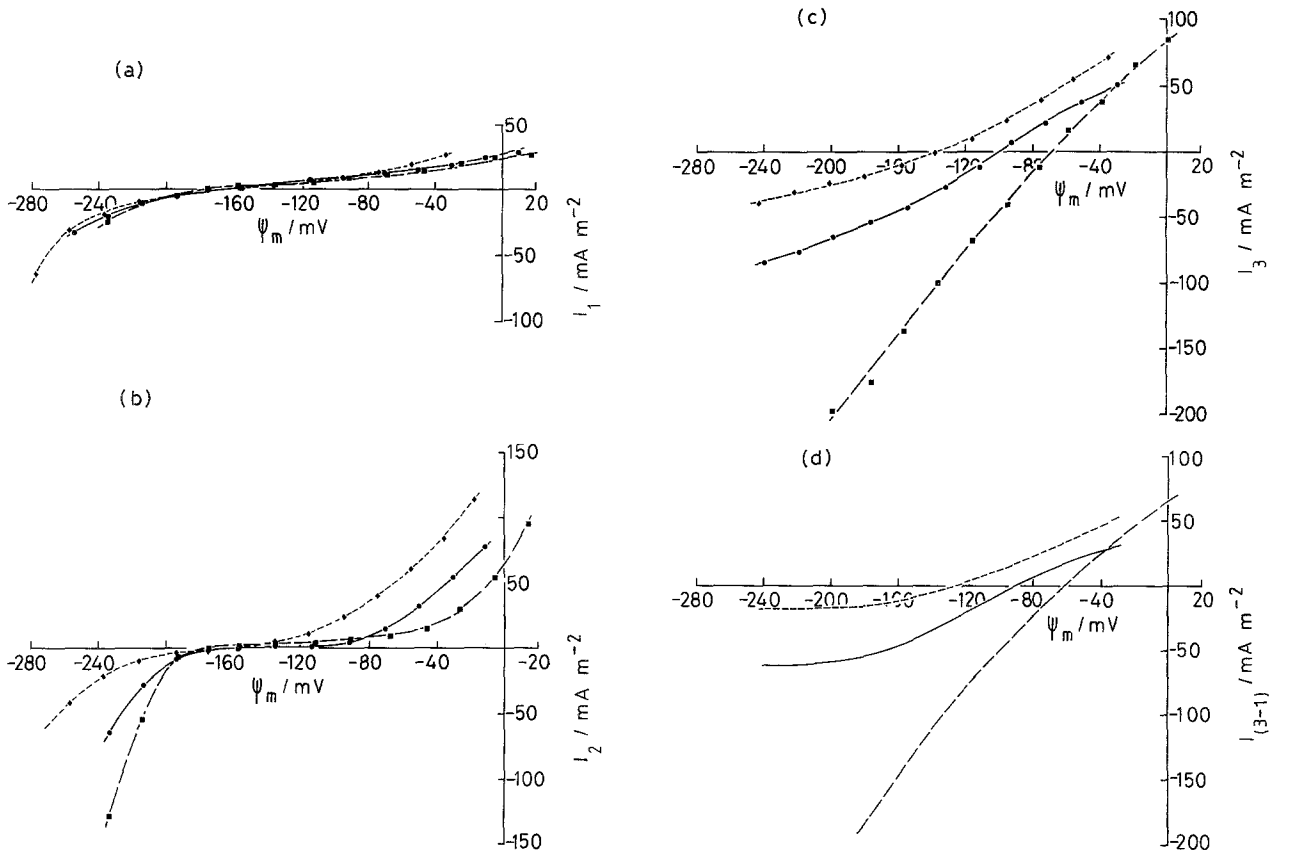

Fig. 4. (*a*) $I_1 \sim \psi_m$, (*b*) $I_2 \sim \psi_m$, (*c*) $I_3 \sim \psi_m$, (*d*) $(I_1 - I_3) \sim \psi_m$, all as functions of $[K^+]_o$: (♦) 0.1 mM, (●) 1.0 mM, (■) 10.0 mM. The curves have been fitted by eye in (*a*) – (*c*), and the difference between these fitted curves of $I_3 \sim \psi_m$ and $I_1 \sim \psi_m$ are shown in (*d*)

Table. Electrical parameters of the *Hydrodictyon* membrane

$[K^+]_o$ (mM)	PD (mV)		Conductances (S m^{-2})				Concentrations (mM)
	$(\psi_m)_{I_2=0}$	$(\psi_m)_{I_3=I_1}$	$(\partial I_2/\partial \psi_m)_{I_2=0}$	$(\partial I_1/\partial \psi_m)_{I_3=I_1}$	$(\partial I_3/\partial \psi_m)_{I_3=I_1}$	$(\partial (I_3-I_1)/\partial \psi_m)_{I_3=I_1}$	$[K^+]_{i\,calc}$
0.1	−178±6(16)[a]	−137±10(5)	0.12±0.01(16)	0.12±0.03(5)	0.55±0.12(5)	0.43±0.11(5)	24.9
1.0	−167±9(6)	−87±3.5(3)	0.15±0.06(6)	0.09±0.00(3)	0.65±0.13(3)	0.55±0.14(3)	40.1
3.0	−117±19(4)	−49(50, −48)[b]	0.13±0.05(4)	0.14(0.13, 0.15)[b]	0.68(1.0, 0.37)[b]	0.54(0.87, 0.22)[b]	27.7
10.0	−111±36(3)	−43(−23, −63)[b]	0.11±0.07(3)	0.18(0.26, 0.10)[b]	1.12(0.80, 1.44)[b]	0.94(0.54, 1.34)[b]	65.9

[a] Result given here, and elsewhere in the paper as mean ±SEM with the number of observations in brackets.
[b] Mean of only two values (given separately in brackets).

ery phase of ψ_m at the end of the step. For $[K^+]_o$ = 0.1 mM, the initial peak in ψ_m still occurs but the recovery at the end of the pulse does not show an obvious plateau (Fig. 5*b*).

The effects of varying the duration of current pulses large enough to produce the initial peak in ψ_m, are shown in Fig. 5*c*. For the shortest pulse shown, the plateau is barely discernable, but becomes more apparent as the pulse duration is increased.

We have also examined the response of ψ_m to positive and negative current pulses in cells where the membrane was not hyperpolarized, or only hyperpolarized to some extent; *see* Fig. 5*d*. A threshold is discernable, and when ψ_m moves below this threshold (for negative current pulses) there is a further increase in the change in ψ_m.

Effects of TEA^+ and C_9^+: Voltage-Clamp Data

The TEA and C_9 (nonyltriethylammonium) ions are known to block potassium channels in nerve

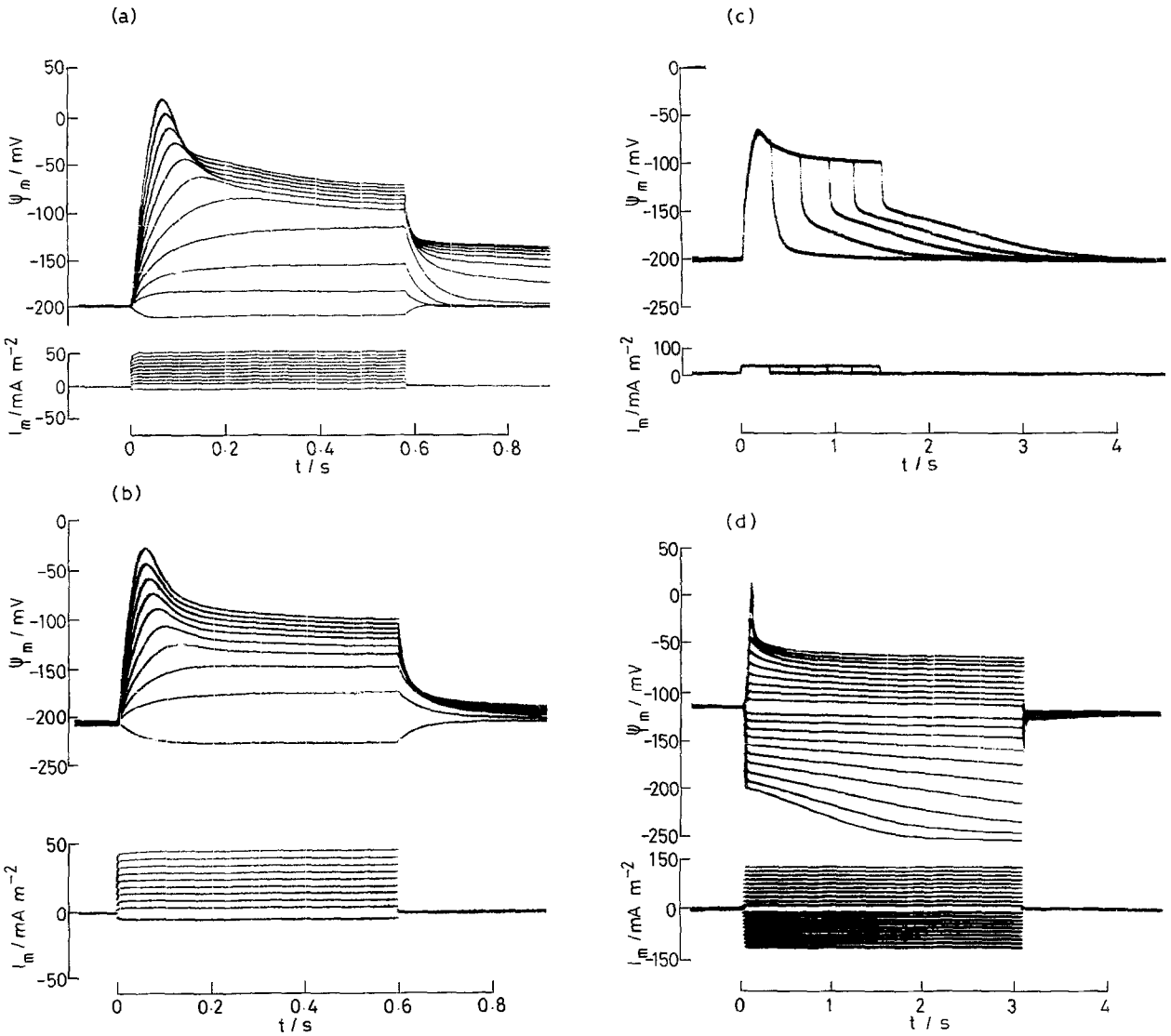

Fig. 5. (*a*) Response of ψ_m (upper traces) to a series of constant-current steps of differing magnitudes. $[K^+]_o = 1.0$ mM. (*b*) As for (*a*), but with $[K^+]_o = 0.1$ mM. (*c*) Response of ψ_m to a series of constant-current pulses of the same magnitude but different duration. $[K^+]_o = 1.0$ mM. The results shown in (*a*) – (*c*) are from the one cell. (*d*) Response of ψ_m to a series of constant-current steps of differing magnitudes. $[K^+]_o = 1.0$ mM. In this cell the membrane was unhyperpolarized with a resting value of ψ_m of −115 mV. *See* text for further details

membranes (Armstrong, 1971). We tested their effects on the *Hydrodictyon* membrane because Findlay (1982) has shown that there are good reasons for believing that some of the transient electrophysiological behavior of this membrane can be ascribed to transients in the potassium conductance g_K and by inference, opening and closing of potassium channels.

The addition of 10 mM TEA^+ to the external bathing medium considerably diminished the S-shaped rise in I_m for voltage-clamped steps in ψ_m, for values less negative than ψ_{th}; *see* Fig. 6*a*. The effects of TEA^+ on the $I \sim \psi_m$ curves are shown in Fig. 6*b*. The addition of 1 mM C_9^+, externally, completely eliminated the rise in I_m for voltage-clamp steps; Fig. 6*c*. The effects of TEA^+ were reversible, with cells returning to their control state within 30 min of removal of TEA^+, but the effects of C_9^+ were not reversible and continued for many hours after the removal of C_9^+ from the bathing medium.

Effects of TEA^+: The Free-Running Membrane PD

The response of ψ_m to positive current pulses, for $[K^+]_o = 1.0$ mM, with and without 10 mM TEA^+ is shown in Fig. 7*a*. The presence of TEA^+ had

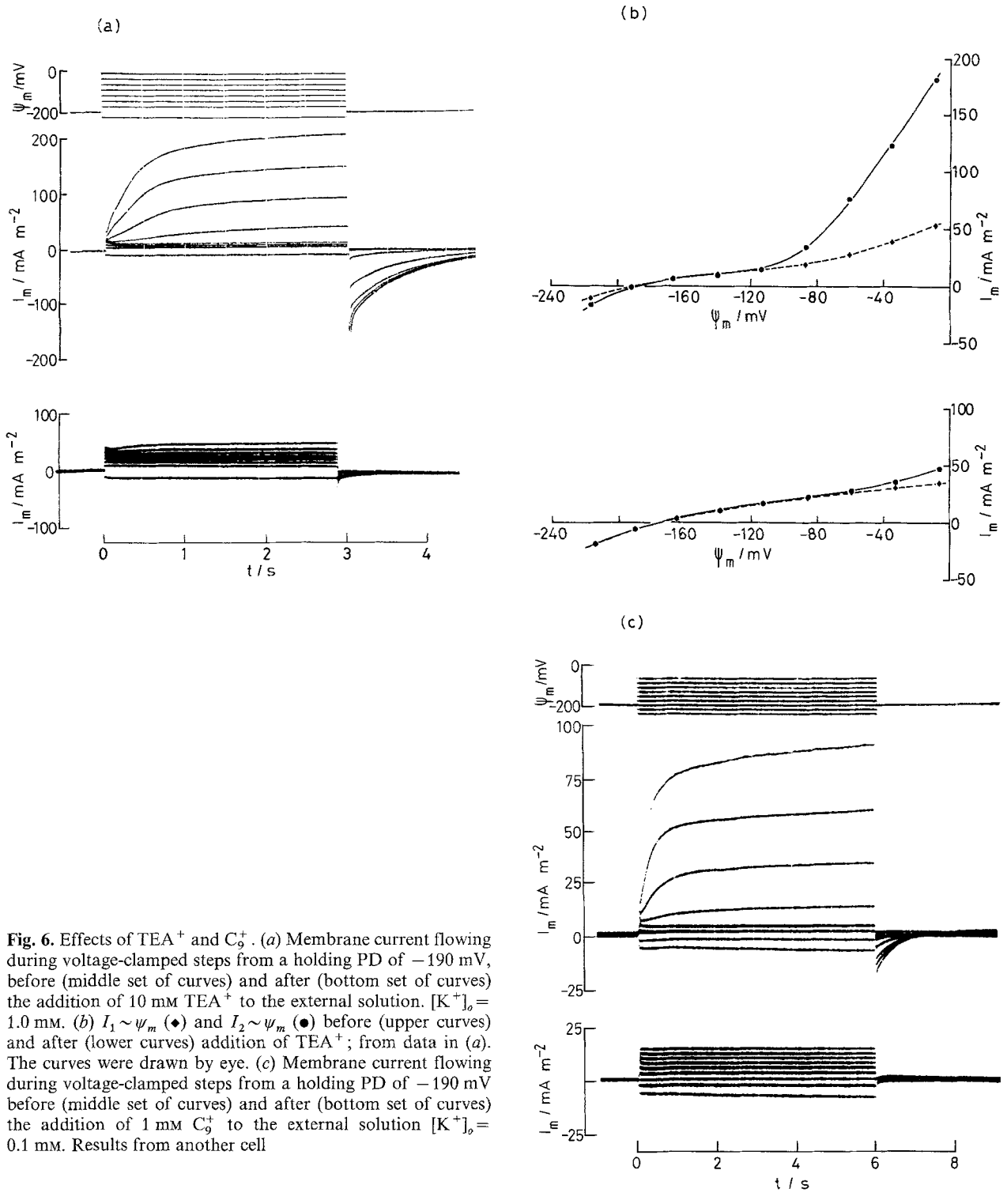

Fig. 6. Effects of TEA^+ and C_9^+. (*a*) Membrane current flowing during voltage-clamped steps from a holding PD of −190 mV, before (middle set of curves) and after (bottom set of curves) the addition of 10 mM TEA^+ to the external solution. $[K^+]_o$ = 1.0 mM. (*b*) $I_1 \sim \psi_m$ (♦) and $I_2 \sim \psi_m$ (●) before (upper curves) and after (lower curves) addition of TEA^+; from data in (*a*). The curves were drawn by eye. (*c*) Membrane current flowing during voltage-clamped steps from a holding PD of −190 mV before (middle set of curves) and after (bottom set of curves) the addition of 1 mM C_9^+ to the external solution $[K^+]_o$ = 0.1 mM. Results from another cell

little effect on the initial rise of ψ_m but the initial peak was largely eliminated, and at the cessation of the pulse the plateau was absent.

In cells where the membrane was unhyperpolarized, the addition of 10 mM TEA^+ to the external bathing solution often produced the change in ψ_m as shown in Fig. 7*b*. After the application of TEA^+ a decrease in the total membrane conductance g_m accompanied the change in ψ_m to the more negative value.

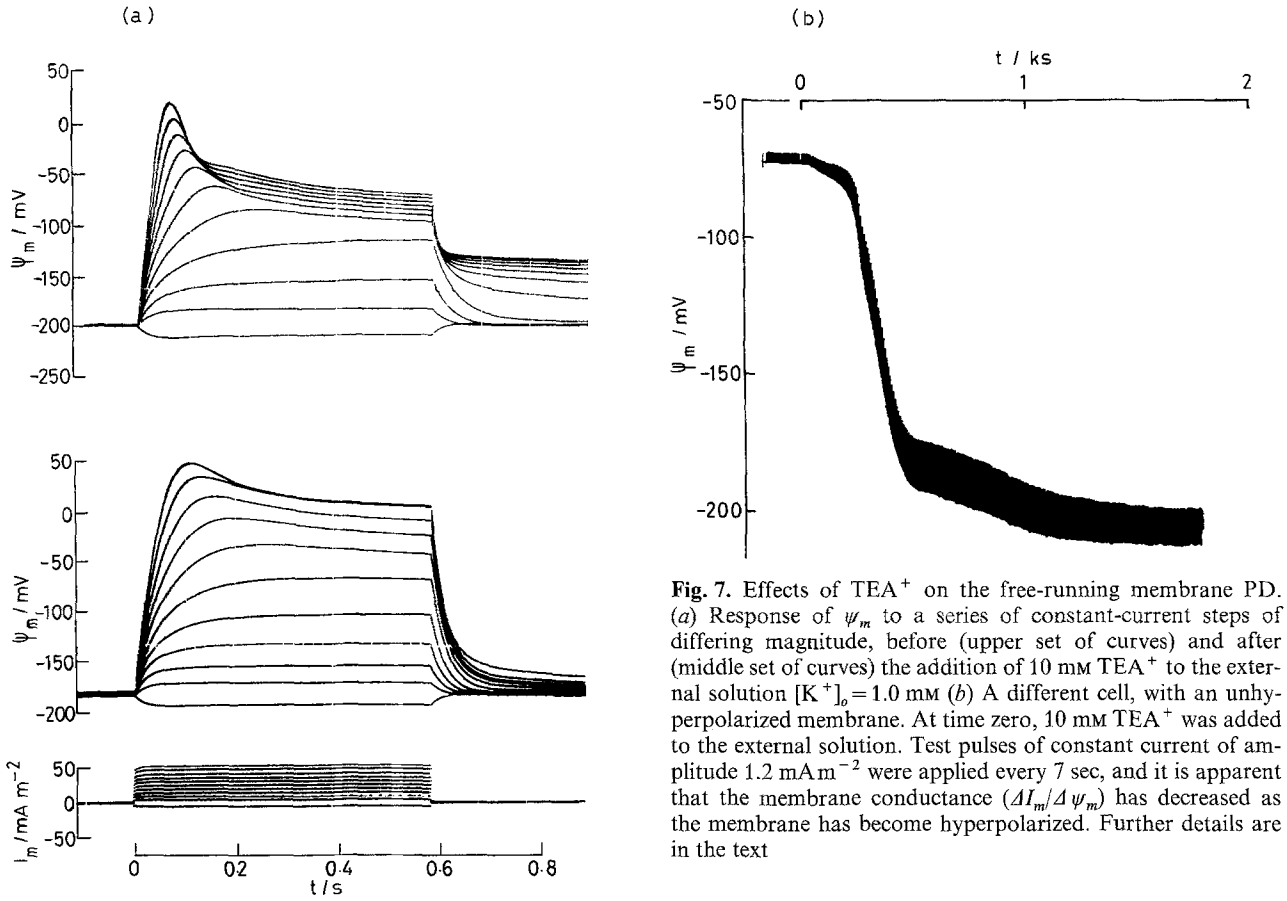

Fig. 7. Effects of TEA^+ on the free-running membrane PD. (*a*) Response of ψ_m to a series of constant-current steps of differing magnitude, before (upper set of curves) and after (middle set of curves) the addition of 10 mM TEA^+ to the external solution $[K^+]_o = 1.0$ mM (*b*) A different cell, with an unhyperpolarized membrane. At time zero, 10 mM TEA^+ was added to the external solution. Test pulses of constant current of amplitude 1.2 mA m^{-2} were applied every 7 sec, and it is apparent that the membrane conductance ($\Delta I_m/\Delta\psi_m$) has decreased as the membrane has become hyperpolarized. Further details are in the text

Discussion

Voltage-Clamp Data

This paper presents evidence for the existence of time- and potential-dependent channels, carrying potassium ions, in the membrane of *Hydrodictyon africanum*. The results can account for the variable potassium conductance described by Findlay (1982) and also provide information about the kinetics of opening and closing of the channels.

The clamp currents in *Hydrodictyon,* as shown in Fig. 1, have a shape very similar to that in excitable membranes of animals such as the squid (Hodgkin & Huxley, 1952; Armstrong, 1975) but occur on a time scale of seconds, rather than milliseconds. On the other hand, the clamp currents in *Hydrodictyon* have a time course very similar to that recorded in artificial phospholipid membranes with added antibiotics such as monazomycin (Muller & Finkelstein, 1972). Recent work with patch clamps has shown that for both the squid axon (Conti & Neher, 1980) and the phospholipid membrane with added monazomycin (Muller & Andersen, 1982) the observed potassium currents arise directly from the opening and closing of a large number of discrete channels. It seems quite likely that the S-shaped clamp current in *Hydrodictyon* is carried through similar discrete channels. The evidence that known blockers of K^+ channels in nerve membranes, such as TEA^+ and C_9^+ (Armstrong, 1975) also eliminate this current in *Hydrodictyon,* together with the observed effects of changes in $[K^+]_o$ on these clamp currents, as shown in Fig. 4, and discussed later, strongly suggest that the current is carried predominantly by K^+ and that the inferred channels in the *Hydrodictyon* membrane are potassium channels.

When the electrogenic transport of H^+ is operating in the *Hydrodictyon* membrane (Findlay, 1982) and holding ψ_m at a sufficiently negative value, the K^+ channels, or at least a major fraction of them, are closed. The channels open when ψ_m rises above a threshold value. The channel opening, as indicated by the currents in response to voltage-clamped steps in ψ_m is not instantaneous and produces the characteristic time course of the current as shown in Fig. 1. Although in some cells

the current rises to a steady value after a few seconds, usually there was a continuing slower rise for longer periods.

Channels which are opened by positive-going steps in ψ_m, can be closed either partially or fully by a subsequent negative-going step in ψ_m, either to the original holding PD or at least to a value below the threshold; *see* Figs. 1 and 2. The closing of the channels is not instantaneous, and is manifest by a declining current or "tail" commencing from the start of the negative step. The potassium current I_K flowing across the membrane will be given by $I_K = g_K(\psi_m - \psi_K)$ where g_K is the potassium conductance, and ψ_K the Nernst potential for K^+. The reversal of the clamp current at the end of the positive step is caused by a change in sign of $(\psi_m - \psi_K)$. Because $(\psi_m - \psi_K)$ is constant, the bunching up of the tails indicates that g_K tends to a maximum value as the magnitude of the positive step in ψ_m is increased. As the holding PD is made more negative, the magnitude of the tails increases because the magnitude of $(\psi_m - \psi_K)$ is increased. The double-pulse experiments (Fig. 2) show that the rate of closing of the channels increases as ψ_m is made more negative.

Current-PD Curves

The instantaneous current I_1 represents the current flowing through pump and diffusive components of the membrane before the onset of opening of the K^+ channels. Even if we assume that the $I_1 \sim \psi_m$ curve remains unchanged during K^+ channel opening, it is clear that I_1 forms an appreciable component of the total membrane current and must be taken into account in estimating the current-PD characteristics of the membrane caused by channel opening, and any other time- and PD-dependent changes which may occur. In comparison, the leak current in the squid axon is very small compared to both Na^+ and K^+ currents (Hodgkin & Huxley, 1952).

In the double-step experiment, the prepulse was chosen to produce maximum channel opening. At the end of the prepulse, the channels do not close instantaneously, and thus the $I_3 \sim \psi_m$ curve (Fig. 4*c*) should be the current-PD curve for the membrane with open K^+ channels and the $(I_3 - I_1) \sim \psi_m$ curve the current-PD curve for the open channels alone, assuming that the $I_1 \sim \psi_m$ curve remains unchanged during channel opening. For $(\psi_m)_{I_3 = I_1}$, the component of membrane conductance due to the open K^+ channels, and given by $\partial(I_3 - I_1)/\partial\psi_m$ increases to some extent with increasing $[K^+]_o$, ranging from about 3× the instantaneous conductance $(\partial I_1/\partial\psi_m)_{I_3 = I_1}$, for $[K^+]_o = 0.1$ mM, to about 5× when $[K^+]_o = 10.0$ mM. If K^+ is the only ion moving in the channel, then $I_3 - I_1 = I_K = g_K(\psi_m - \psi_K)$, where ψ_K is the Nernst PD and given by $\psi_K = 58 \log([K^+]_o/[K^+]_i)$. Thus when $(I_3 - I_1) = 0$, $\psi_m = \psi_K$. From the data (Table and Fig. 4*d*) it can be seen that the values of ψ_m for $(I_3 - I_1) = 0$ show a strong K^+ dependence, although they do not vary with $[K^+]_o$ strictly in accordance with the Nernst equation. A number of factors might produce this discrepancy. The channels may not be completely selective for K^+, or there may be significant changes in cytoplasmic $[K^+]$ during the course of an experiment. Estimates of $[K^+]_i$ obtained by using the values of ψ_m for $(I_3 - I_1) = 0$ generally were higher than the measured vacuolar concentrations, but still less than the values expected for the cytoplasmic concentration (Findlay, 1982). Further experiments are needed to examine these problems in more detail.

The steady-state current, I_2, is the current flowing through the membrane after the various time- and potential-dependent changes have occurred. The steeply rising part of the $I_2 \sim \psi_m$ curve for outward currents arises from the increasing fraction of open K^+ channels. Other features of this curve need comment, particularly the very flat part of the curve extending from the vicinity of the resting PD of the cell (where $I_2 = 0$) for about 60 mV. In this region quite small changes in outward membrane current, such as variations in the outward electrogenic H^+ transport (Findlay, 1982) could produce quite large changes in ψ_m.

For small positive steps in ψ_m, the membrane current sometimes showed a decline from its initial value I_1, to the final steady value I_2: *see* Fig. 1. This has the effect of making the $I_2 \sim \psi_m$ curve flatter than the $I_1 \sim \psi_m$ curve. We were inclined initially to think that the fact that the $I_2 \sim \psi_m$ curve lay below the $I_1 \sim \psi_m$ curve for small positive steps in ψ_m, but subsequently crossed the curve and rose more steeply, as the K^+ channels opened, supported Findlay's (1982) suggestion that the threshold for the opening of the K^+ channels was at a value of ψ_m more negative than ψ_K. If this were so, $(I_2 - I_1)$, the component of the membrane current flowing through the K^+ channels, would be negative for ψ_m more negative than ψ_{th} and would change sign when ψ_m is less negative than ψ_K because the driving force on K^+ is a function of $(\psi_m - \psi_K)$. However, this "drooping" of the $I_2 \sim \psi_m$ curve below the $I_1 \sim \psi_m$ curve was not always observed, and in a few cells in which it was observed, no subsequent increased K^+ current oc-

curred. Thus we are not able to locate ψ_{th} with any certainty. Findlay (1982) estimated ψ_{th} as that value of $\psi_m (= \partial I_1 / \partial \psi_m)$ began to rise following its initial decline after the onset of darkness. However, this analysis assumed that no other component of the diffusive pathways appeared as a result of the start of darkness: this assumption may not necessarily be valid.

The $I_2 \sim \psi_m$ curves also rise steeply for inward currents and are produced by time-dependent conductance changes with a time course different from conductance changes for outward current. The curves shown in Fig. 4 suggest that these inward currents are K^+ dependent, but the nature of the current is not known. The data from the double-step experiments do suggest, however, that the inward current is a separate component from the outward current. In Fig. 2*b* in the bottom two-current curves the decay of the K^+ current can be seen preceding the slower changing negative currents.

The almost complete elimination of the channel component of the clamp current by the addition of TEA^+ and C_9^+ provides strong evidence for the existence of K^+ channels in the *Hydrodictyon* membrane. The results shown in Fig. 6 clearly identify the K^+ current, but show that I_1 is largely unaffected by TEA^+ or C_9^+, consistent with the observation that I_1 is largely insensitive to $[K^+]_o$; Fig. 4. In *Hydrodictyon*, C_9^+ acts as a direct blocker of K^+ channels, unlike its effect on the squid giant axon membrane, where it produces an inactivation of the open K^+ channels (Armstrong, 1975). Furthermore, in *Hydrodictyon* C_9 irreversibly blocks K^+ channels, whereas the blocking effect of TEA^+ is reversible.

The Free-Running Membrane

Findlay (1982) has described various aspects of the free-running membrane PD. The voltage-clamp data in this paper allows us to make a more detailed analysis. The responses of ψ_m to pulses of constant current, as shown in Fig. 5*a*, result from a complex series of events and we will consider each in turn. The resting PD of the membrane is ~ -175 mV, and so the membrane is hyperpolarized because $\psi_K \simeq -80$ to -120 mV for $[K^+]_o =$ 1.0 mM. Hence the proton extrusion pump must be operating. For the first three positive pulses there is an approximately exponential rise and fall in ψ_m, with the values of ψ_m lying on the $I_1 (= I_2) \sim \psi_m$ curve. For the fourth and subsequent pulses, ψ_m has been taken over the threshold level ψ_{th}, and g_K rises, but not instantaneously. The effect of this increase in g_K is to cause ψ_m to move from its initial position on the $I_1 \sim \psi_m$ curve, to a more negative value on the $I_2 \sim \psi_m$ curve. As the current pulses are increased in magnitude ψ_m initially will move further along the $I_1 \sim \psi_m$ curve, and approaches its final value at a rate determined by the membrane conductance and capacitance. As well, the rate at which the membrane current $\sim$ PD curve changes from $I_1 \sim \psi_m$ to $I_2 \sim \psi_m$ increases as ψ_m becomes more positive and the combined effect will cause the initial peak in ψ_m to occur earlier. Immeditely prior to the end of the pulse the current-PD curve for the membrane will be close to the $I_2 \sim \psi_m$ curve; the smaller spacing between each ψ_m response merely reflects their location on the steep part of the $I_2 \sim \psi_m$ curve.

The fraction of open channels increases as ψ_m become less negative, and consequently the $I_3 \sim \psi_m$ curve moves to the right, becomes steeper and approaches a final position when the fraction of open channels is a maximum. Thus the intercept of the $I_3 \sim \psi_m$ curve with the zero current axis will tend to a least negative value of ψ_m. At the cessation of the current pulses (Fig. 5*a*) g_K will be elevated, and the membrane characteristics will be determined approximately by the $I_3 \sim \psi_m$ curve. Thus ψ_m will move to a value determined by the intersection of the $I_3 \sim \psi_m$ curve with the zero current axis. This accounts for the bunching up of the ψ_m values, after the end of the current pulse, as the magnitude of the current pulse (and the resultant step in ψ_m) increases, and is equivalent to the bunching up of the current tails at the end of the voltage-clamp steps (Fig. 1). In effect, ψ_m at the end of the current pulses tends towards ψ_K. For $[K^+]_o = 0.1$ mM (Fig. 5*b*), ψ_K is much closer to the membrane resting PD and the plateau after the end of the pulse is less easily seen.

The recovery of ψ_m is caused by two factors, first the presence of H^+ pump activity (Findlay, 1982) tending to hyperpolarize the membrane and bring ψ_m below ψ_{th} and secondly the time and PD dependence of g_K. The change in ψ_m to a more negative value at the end of the current pulse causes g_K to decline and the membrane characteristics to revert to control by the $I_2 \sim \psi_m$ curve; eventually ψ_m returns to the original resting level. The larger the fraction of K^+ channels open, the longer g_K will take to decline, and the longer will be the recovery of ψ_m to its resting level. This is particularly evident in Fig. 5*c*, where only for the longer pulses has g_K approached its increased steady level before the end of the pulse. Factors which prevent the opening of the potassium channels will eliminate many of the changes in ψ_m describe above,

and the response of ψ_m to current pulses will be determined largely by the $I_1 \sim \psi_m$ characteristics of the membrane. This is observed in cells in the presence of TEA^+ as shown in Fig. 7*a*, where the initial peaks have almost disappeared except for the largest step in I_m, and there is no plateau after the end of the current pulse.

Occasionally cells of *Hydrodictyon* are in a less hyperpolarized steady state, and the data of Fig. 5*d*, show that the reason for this, at least in part, is that the potassium channels are partially open. These channels are still capable of further opening, and can also be closed when ψ_m is made more negative. Alternatively, if the potassium channels are closed by some other means, and we have done this by applying TEA^+ (Fig. 7*b*), the membrane will return to its hyperpolarized state, indicating that the pump was operating, even though the K^+ channels were open.

This project has been supported, financially, by the Australian Research Grants Scheme.

References

Armstrong, C.M. 1971. Interaction of tetraethylammonium ion derivatives with the potassium channels of giant axons. *J. Gen. Physiol.* **58**:413–437

Armstrong, C.M. 1975. Ionic pores, gates and gating currents. *Q. Rev. Biophys.* **7**:179–210

Bielby, M.J., Coster, H.G.L. 1979. The action potential in *Chara corallina*. II. Two activation-inactivation transients in voltage clamps of the plasmalemma. *Aust. J. Plant Physiol.* **6**:323–335

Conti, F., Neher, E. 1980. Single channel recordings of K^+ currents in squid axons. *Nature (London)* **285**:140–143

Findlay, G.P. 1982. Electrogenic and diffusive components of the membrane of *Hydrodictyon africanum*. *J. Membrane Biol.* **68**:179–189

Findlay, G.P., Hope, A.B. 1964. Ionic relations of cells of *Chara australis*. VII. The separate electrical characteristics of the plasmalemma and tonoplast. *Aust. J. Biol. Sci.* **17**:62–77

Findlay, G.P., Hope, A.B. 1976. Electrical properties of plant cells: Methods and findings. *In:* Encyclopedia of Plant Physiology, New Series, Vol. 2. Part A, Transport in Plants II. pp. 53–92. U. Lüttge and M.G. Pitman, editors. Springer-Verlag, Berlin – Heidelberg – New York

Hill, S.A., Osterhout, W.J.V. 1938. Calculations of bioelectric potentials. II. The concentration potential of KCl in *Nitella*. *J. Gen. Physiol.* **21**:541–556

Hodgkin, A.L., Huxley, A.F. 1952. Currents carried by sodium and potassium ions through the membrane of the giant axon of *Loligo*. *J. Physiol. (London)* **116**:449–472

Keifer, D.W., Lucas, W.J. 1982. Potassium channels in *Chara corallina*. Control and interaction with the electrogenic H^+ pump. *Plant Physiol.* **69**:781–788

Muller, R.U., Anderson, O.S. 1982. Monazomycin induced single channels. II. Origin of the voltage dependence of the macroscopic conductance. *J. Gen. Physiol.* **80**:427–449

Muller, R.U., Finkelstein, A. 1972. Voltage-dependent conductance induced in thin lipid membranes by monazomycin. *J. Gen. Physiol.* **60**:263–284

Osterhout, W.J.V. 1930. Calculations of bioelectric potentials. I. Effects of KCl and NaCl on *Nitella*. *J. Gen. Physiol.* **13**:715–732

Smith, P.T., Walker, N.A. 1981. Studies on the perfused plasmalemma of *Chara corallina*. I. Current-voltage curves: ATP and potassium dependence. *J. Membrane Biol.* **60**:223–236

Received 18 January 1983; revised 9 March 1983